Measurement of Pyrophosphate Concentration in Cells by Simple Terpyridine-Zn(II) Probe

Gunjan Pandey
Master's Thesis
University of Jyväskylä
Department of Biological and Environmental Science
Cell and Molecular Biology
30.10.2015

Preface

I am incredibly thankful to my supervisors (from Biology to Chemistry):

Varpu Marjomäki for providing me the opportunity to work on this Master's thesis topic under her able mentor ship. **Kari Rissanen** for being the backbone and orchestrating the smooth workflow throughout the project. With adept guidance of **Sandip Bhowmik,** I understood the intricately connected chemical transfigurations occurring inside the cell. *Varpu's* amazing knowledge in the field of Cell Biology complemented by *Sandip's* background in Organic Chemistry added up to my understanding.

I am grateful to *Maria Pellicia* for building my foundation in the science of cell culture. *Kanoktip Thammasari,* for clarifying sudden bursts of random doubts.

I shall like to convey my regards to *Marie Stark, Artur Kazmertsuk, Mira Myllynen, Nina Rintanen, Mari Martikainen, Moona Huttunen, Anni Honkimaa, Paula Turkki, Rakesh Puttreddy, Lassi Paavolainen* for creating a warm and convivial working atmosphere.

I am also thankful to *Julia Marjomäki* and *Siddharth Dixit* for their help to sculpt the final layout of the thesis.

University of Jyväskylä
Faculty of Mathematics and Science

Abstract of Master's Thesis

Author	Gunjan Pandey
Title	Measurement of Pyrophosphate Concentration in Cells by Simple Terpyridine-Zn(II) Probe
Date	30.10.15 **Pages**: 42
Department	Department of Biological and Environmental Science
Chair	Cell and Molecular Biology
Supervisors	Varpu Marjomäki, Kari Rissanen, Sandip Bhowmik

Abstract:

Pyrophosphate (PPi) anion is an integral part of our physiology. It partakes in the crucial energy transactions in cells and proffers energy for the harmonious functioning of the cell machinery. Discrepancies in PPi concentrations have been associated with several pathological aberrations such as chronic pyrophosphate arthropathy, calcium pyrophosphate deposition disease, cancer etc. However, there still exists a strong demand for an efficient and specific cell based assay for PPi in order to tap its importance to full potential.

Terpyridine-Zn^{2+} complex ($ZnCl_2L$ probe) binds with PPi in 1:3 stoichiometry. This association engenders an emission band (λ_{em}) at ~591 nm when excited at 440 nm with spectrophotometer. It has lowest detection limit (LOD) of 0.8 nM. Water media based, ultra sensitive detection attribute of fluorescent chemosensor $ZnCl_2L$ probe was implemented to investigate pyrophosphate concentrations. In addition to that available commercial kits from *Life Technologies, Lonza & Abcam* manufacturers were also used for comparison. The probe showed remarkable detection ability for PPi. It generated a linear curve from 0-13.32 μM concentration. Higher concentration (>50 μM) of probe solution should be implemented in order to test PPi concentrations higher than 13.32 μM. The measured pyrophosphate content with the probe in cells was found to be in micromolar range. Contribution of interference from other molecules still remains to be tested. The stability of the PPi-probe-complex was tested against several time points, and was found stable until 24 hr time point. Intense reddish-orange fluorescence in cells stained with $ZnCl_2L$ probe under confocal microscope setup confirmed the phenomenon.

In conclusion, the $ZnCl_2L$ probe proved to offer a reliable method to measure PPi. It could hopefully be used to make measurements from various body fluids. Thus, PPi analysis may assist in diagnosis of diseases where increased levels of PPi are present.

Keywords: Pyrophosphate (PPi), $ZnCl_2L$ probe, Cell homogenates, Fluorescence, Commercial kits

Table of Contents

Abbreviations

PPi	Pyrophosphate
Pi	Inorganic Phosphate
$ZnCl_2$.L probe /Probe	$ZnCl_2$**L**, L = 4'-(*N*,*N*'-dimethylaminophenyl)-2,2':6',2''-terpyridine
GMK	Green Monkey Kidney cells
HeLa MZ	Henrietta Lacks
A549	Adenocarcinoma Human Alveolar Basal Epithelial Cell line
BHK	Baby Hamster Kidney Cells
MDA MB 231	Mammary gland/ Breast derived adenocarcinoma from metastatic site
HEP G2	Hepatocellular Carcinoma cell
RF	Rat Fibroblasts
MF	Mouse Fibroblasts
HUVEC	Human Umbilical Vein Endothelial cells
Pr HUVEC	Primary Human Umbilical Vein Endothelial cells
DMEM	Dulbecco's Modified Eagle Medium
MEM	Eagle's Minimum Essential Medium
BSA	Bovine Serum Albumin
ATP	Adenosine Triphosphate
NTPPPH	Nucleoside triphosphate pyrophosphohydrolase
RT	Room Temperature
Ctrl	Control
Std	Standard

1. Introduction

1.1 What is Pyrophosphate (PPi)?

Amongst complex compounds of phosphorus, pyrophosphate (PPi) has intricate involvement in several metabolic aberrations such as osteoarthiritis and hypophosphatasia (for review see Terkeltaub *et al.,* 2001). Pyrophosphates exhibit the highest level of water solubility compared to other phosphates in their family. Symbolically PPi is represented as $(P_2O_7)^{4-}$. In 1970's, it was considered that the elevated hydrolysis efficiency of *pyrophosphatase* decreased PPi levels in the cells (Klemme, 1976). Later on, with the accrual of more reports highlighting the significant intracellular pyrophosphate concentration led to their extensive study. Research comprehending the fate and impact of PPi at intra and intercellular levels dawned in the following decade. Phosphorous can be found in the backbone of DNA, RNA and in ATP in the cellular framework. Depending on the demands of the living system, pyrophosphate linkages known as phosphodiester bonds are broken to release energy. Such hydrolysis of ATP can occur by two ways (Fig. 1). Phosphoanhydride bonds produce 7.3 kcal/mol energy.

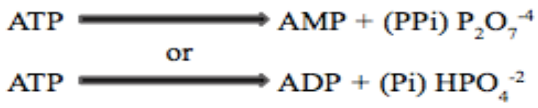

Fig. 1 Equations representing formation of PPi and Pi from ATP

1.2 Pyrophosphate *in vivo*:

The studies done so far indicated cytosol to be the major reservoir of PPi in cells with minor amounts in mitochondria (for review see Caswell *et al.*, 1983a). The complex-forming property of PPi allows it to participate in several intracellular events. It can affect the activity of ATPases, participate in DNA replication, assist in Fe-transfer and delivery, act as phosphate donor in phosphorylation reactions etc. (for review see Terkeltaub *et al.,* 2001). In mammals, PPi is obtained by internal metabolic activities. It is not supplemented via dietary components or by de novo synthesis (for review see Caswell *et al.*, 1983a; Terkeltaub *et al.,* 2001). Some of the researches presenting the PPi content in cell-based analysis are combined together and presented in Table 1.

Table 1 PPi concentrations obtained by various researchers in different cell types in varying conditions.

Sample type	PPi Concentration
Skin Fibroblasts (Lust *et al.,* 1976)	322±66 *pmol*/10^6*cells*
Chondrocytes (Lust and Seegmiller 1976)	131±9 *pmol*/μg DNA
Chondrocytes (McGuire *et al.,* 1980)	457±60 *pmol*/μg DNA
Chondrocalcinotic Fibroblasts (Lust *et al.,* 1981)	400±80 *pmol*/10^6cells
Simian Fibroblasts (Terkeltaub *et al.,* 1994)	50 *pmol*/μg protein
Human Chondrocytes (Lotz *et al.,* 1995)	62 *nmol*/μg protein

Apart from the intracellular reaction mechanisms, pyrophosphate can be found in synovial fluid, blood plasma and urine in regulated amounts. Extra-cellular PPi is the outcome of several factors, such as release of PPi from the cells in case of cell death or injury, enzymatic activity of adenylate cyclase, PPi generation by Nucleoside triphosphate pyrophosphohydrolase (NTPPPH) present within the membrane (Ryan *et al.* 1986), and polarity dependent transport of PPi to sub-chondral bone (Caswell *et al.*, 1983a). The PPi values in the tissues change depending on the controlling mechanism operational in particular location (Caswell *et al.*, 1983a; Terkeltaub *et al.,* 2001). Some values demonstrating the levels of extra-cellular PPi have been documented (Table 2).

Table 2 PPi concentrations obtained by various researchers in extra-cellular regions.

Sample type	PPi Concentration
Synovial Fluid (Michael *et al.,* 1981)	3.5 μM
Plasma (Russell *et al.,* 1970)	1.19-5.65 μM
Bone (Alfrey and Solomons, 1976)	0.36 mg/g

PPi functions as a feedback regulator along with inorganic phosphate to inhibit mineralization of calcium pyrophosphate crystal and hydroxyapatite. Levels of PPi are different in each individual (Armstrong *et al.*, 1975, Heinonen, 2001). Appropriate removal of excess extra-cellular PPi is important to maintain homeostasis and avoid development of pathological conditions. Elevated PPi levels lead to e.g. osteogenesis imperfecta (Armstrong *et al.*, 1975) and osteoarthritis (Cong *et al.*, 2002; Florence *et al.*,

2012). Hypophosphatasia is one of several known examples where dysfunctioning of inorganic pyrophosphatase results in increased extra-cellular PPi content due to higher calcium pyrophosphate crystal deposition (CPPD) deposition in articular cartilages (for review see Terkeltaub *et al.,* 2001). Other such instances include chronic renal failure, which results in increased PPi amounts in bones, serum and plasma (for review see Terkeltaub *et al.,* 2001). Renal stones could be formed in cases of improper urinary PPi excretion. Plasma PPi deregulation has been associated in cases of osteomalacia, acromegaly, and rheumatoid arthritis (for review see Terkeltaub *et al.,* 2001). Due to its importance in several pathological states it is important to be able to measure its cellular and tissue levels correctly

1.3 Evolution of PPi Measurement Methods:

PPi contents have been investigated in prokaryotes, plants, guinea pigs, rats, dogs and humans. Heinonen *et al.* (1982) first reported 0.5 mM PPi in *E.coli,* the most extensively studied subject. Paper chromatography technique was used to separate PPi from radioactive labeled phosphates. Later, author rectified the value to be 1.3 mM instead of previously mentioned 0.5 mM. This variation in the results was ascribed due to improper chromatographic separation of the target compound during the first set of experiment (Kukko and Heinonen 1982).

Several methods such as colorimetric, enzymatic and probes sensing PPi directly, have been used to study pyrophosphate. Pivotal assays were based on extraction of PPi from the sample of interest for instance cells, tissues etc. by chemical precipitation and chromatography (Heinonen, 2001). PPi has a turnover time of less than half a second, which made it essential to quickly inhibit its production and perform extraction for accurate assessment (Heinonen, 2001). This was achieved by lysing the cells by several ways such as using trichloroacetic acid, formic acid, mixing cells in equal volume of hot phenol buffered with Tris, application of perhloric acid by separating cells on membrane filter in freon cooled with solid carbon dioxide or by rapid freezing leading to quenching of metabolism (Heinonen, 2001). The issue of 5-phosphoribosyl-1-phosphate reported to hydrolyze to ribose-5-phosphate and PPi in acidic conditions was solved by addition of alkali (Heinonen, 2001).

A colorimetric method was developed which was based on blue-green complex formation of PPi in acidic conditions in the presence of molybdate and –SH compounds. Despite improving the method by using mercaptoethanol as the only reductant and precipitating phosphomolybdate with triethylamine, samples were contaminated by inorganic phosphate, which formed phosphomolybdate flocculent henceforth reducing PPi levels (Heinonen, 2001). Ion exchange chromatography based separation of PPi from Pi was implemented in order to increase the sensitivity of the assay. (Heinonen, 2001). In radioactive methods cells were cultured by labeling them with radioactive orthophosphate followed by extraction of the compounds using chromatographic methods (Heinonen, 2001). Precautions and hazards accompanying radioactive substance usage made it less favored technique. Irrespective of the several modifications implemented to attain coherent results, inexplicable differences in the orders of magnitude persisted in the PPi content reported by the earlier authors (Kukko and Heinonen 1982).

In addition to the earlier mentioned assays, more sensitive sensors were produced. Some of them are based on discerning fluorometric signals equivalent to PPi amounts while others have Electrogenerated Chemiluminescence (ECL) proportional to PPi content in sample solution. Shin *et al.* (2010) mentioned the usage of orthogonally bonded ECL reporter (boron dipyromethane) and PPi receptor (phenoxo-bridged bis-Zn^{2+}-dipicolylamine complex). Here, Shin *et al.* (2010) used Zn to produce ECL in acetonitrile solution. It resulted from excited molecules on the electrode surface by an electron transfer redox reaction between redox precursors (Shin *et al.,* 2010). They controlled the system by electrochemistry and not by external light. Other formulations in this area encompass quinone-fused chromophore electrooptical sensors by Anzenbacher *et al.* (2005). Alternatively emerging systems include colorimetric anion sensor tetra-amidourea derived calix[4]arene, supramolecular anion and π interactions between electron deficient Naphthalene Diimide (NDI) unit based sensor, halogen bonding macrocyclic halo-imidazolium receptors and self assembled hydrogen bound anion with poly squaramide groups (Quinlan *et al.,* 2007; Guha *et al.,* 2010; Rostami *et al.,* 2011; Zapata *et al.,* 2012). These compounds perform well in organic solvents.

Inspired by the applicability of the fluorescence sensors in the biological systems, new sensors were developed which could function in organic-aqueous mixtures such as the quinolone-ligated dinuclear zinc complexes detecting PPi via intra-molecular excimer formation (Mikata *et al.,* 2013). Other advances in the field include PPi detection assay based on the use of fluorophore labeled single-stranded DNA in Aluminium [Al(III)] in 10 mM HEPES media (Su *et al.,* 2013). These sensors due to their coupled PPi binding sites and signal transduction units interfere with the measurements as the binding of PPi induces conformational changes in the polymer or cross-chain interactions (Su *et al.,* 2013). Some of the probes possess slight capability to sense PPi in aqueous solutions but their sensitivity depreciates significantly as the target concentration increases. Nucleic acid based techniques involve fluorescent labeling of the single stranded DNA before the quantitative measurement of PPi could be attained through fluorescence response (Su *et al.,* 2013). Fluorometric kit from *Abcam* (*ab112155*) uses water-based sensor to detect PPi. Most common detection kits such as *P_iPER^{TM} Pyrophosphate Assay Kit* (*Life Technologies*) and PPiLight^{TM} Inorganic Pyrophosphate Assay (*Lonza*) were based on pyrophosphate detection by cascade enzymatic reactions (Fig. 3, 4). These reactions are prone to errors due to their indirect approach.

Among fluorescent sensors, simple terpryidine-Zn^{2+} complex ($ZnCl_2L$ probe) has nanomolar sensitivity towards PPi in water at physiological pH (Bhowmik *et al.,* 2014). Bhowmik *et al.* (2014) observed that the UV-Vis spectra of the complex was characterized by three major peaks at 285 nm, 320 nm and 410 nm which remain largely unperturbed upon addition of different anions such as F^-, Br^-, I^-, $SO4^{2-}$, AcO^-, NO^{3-}, CO_3^{2-}, HPO_4^{2-}, PO_4^{3-} and $P_2O_7^{4-}$ (added as their sodium salts). However a sharp bathochromic shift of 30 nm was accounted in the absorption spectra with marginal color change upon introduction of pyrophosphate. It was accompanied by the reduction in the intensity of 410 nm peak. The same group also found that $ZnCl_2L$ probe's solid-state fluorescence was cogently quenched on mixing them with water (Bhowmik *et al.,* 2014). They accounted ~500 fold increment in the fluorescence intensity at 591 nm on addition of 50 μM PPi. Job plot analysis done by Bhowmik *et al.* (2014) confirmed the binding stoichiometry of 1:3 for PPi: $ZnCl_2L$ probe. The LOD of the probe was found to be ~0.8 nm (Bhowmik *et al.,* 2014).

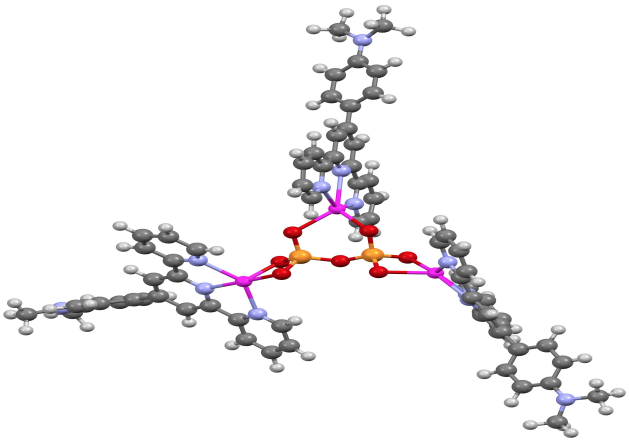

Fig. 2 Energy minimized structure of PPi-$ZnCl_2L$ probe (1:3) complex formation. In grey are the $ZnCl_2L$ molecules. Image Reproduced with permission from Supplementary Information of Bhowmik *et al.* (2014) Nanomolar Pyrophosphate Detection in Water and in a Self-Assembled hydrogel of a Simple Terpyridine-Zn^{2+} Complex

The group marked relatively negligible changes in the presence of nucleotide phosphates in comparison with PPi. The fluorescence intensities of $ZnCl_2L$ probe remained undeterred on addition of 1 equivalents (50 μM) of other anions (Bhowmik *et al.,* 2014) whereas by accretion of 0.001 equivalents (50 nM) of PPi, Bhowmik *et al.* (2014) observed increase in the fluorescence intensity. Noticeable depreciation in PPi's fluorescence was seen due to acute abundance of phosphate anions in presence of HPO_4^{2-} and PO_4^{3-} (Bhowmik *et al.,* 2014). The interference from other untested molecules could also be a factor of concern in the case of cell measurements.

Translucent, irreversible and thixotropic hydrogel was construed from the probe (Bhowmik *et al.,* 2014). Drop casting of PPi solution on disposable paper strips coated with $ZnCl_2L$ hydrogel demonstrated bright orange emission. Conversely they recorded no such emission on application of other anions on the paper gel strip (Bhowmik *et al.,* 2014). By this experiment Bhowmik *et al.* (2014) presented the probe's ability to detect PPi in strip-based assays.

2. Aim of Study

This project was focused on reliable assessment of pyrophosphate content in the cells using the probe ($ZnCl_2L$). The probe was developed in the research group of Kari Rissanen (Bhowmik *et al.,* 2014). Following goals were accomplished during the course of this dissertation:

1) The accuracy and reliability of cellular measurements were compared against the commercially available probes and kits for measuring pyrophosphate.

2) The PPi content in broad spectrum of cells with varying degrees of malignancy was evaluated.

3) In addition to this, stability at different time-points of the produced $ZnCl_2L$ probe-PPi complex was also tested.

3. Material and Methods:

3.1 Cell Culture:

Cell lines used were Green Monkey Kidney Cells (*GMK*), Henrietta Lacks (*HeLa-MZ*), Adenocarcinoma Human Alveolar Basal Epithelial Cell line (*A549*), Mammary gland/ Breast derived adenocarcinoma from metastatic site (*MDA MB 231*), Hepatocellular Carcinoma (*HEP-G2*), Rat Fibroblasts (*RF*), Mouse Fibroblasts (*MF*) and Human Umbilical Vein Endothelial (*HUVEC*) cells. Each cell type was chosen for its unique set of properties. *GMK*s represent the normally proliferating cell types whereas *Hela-MZ*, *A549, MDA MB 231* and *HEP-G2* were from distinct cancerous origin. *Hela-MZ* were derived from the cervical cancer cells from the lab of Marino Zerial, Max-Plank Institute, Dresden. *MDA MB 231* from the metastatic breast cancer anomaly was received from Dr. Johanna Ivaska, University of Turku. *A549*s belonging to lung carcinoma were received from Dr. Petri Susi, University of Turku. The hepatic cancer cells *HEP G2* were obtained from the group of Seppo Ylä-Herttuala, AIV Institute, Kuopio. *RF* and *MF* were the rat and mouse fibroblast cells. They were isolated from rat and mouse muscle tissue by enzymatic digestion in cell culture courses in the year 1998 and 2008 respectively. Mouse fibroblasts were isolated from mouse muscle tissue by Dr Hilkka Reunanen, University of Jyväskylä. A continuous *HUVEC* cell line was received from Merja Roivainen, THL, Helsinki. In this experiment two types of *HUVEC*s were tested one set was passaged from continuous cell line whereas other was from a primary culture.

GMK cells were cultured in 80 cm^2 flat-bottomed flaks (*Nunclon™, USA*) in Eagle's Minimum Essential Medium (*MEM, Gibco Life Technologies, South America*), It was supplemented with 1% Fetal Bovine Serum (*FBS, Gibco Life Technologies, UK*), 1% L-Glutamine (*Gibco Glutamax™, South America*) and 1% Penicillin-Streptomycin antibiotics. Flasks were incubated at 37°C with 5% CO_2 flow (*Thermo Scientific HeraCell 150i, USA*).

Hela-MZ, A549, MDA MB 231, HEP G2, RF, MF and *HUVEC*s (derived from continuous cell lines) were grown with the similar technique but in Dulbecco's Modified Eagle Medium (*DMEM, Gibco Life Technologies, South America*), supplemented with 1% Fetal Bovine Serum (*FBS, Gibco Life Technologies, UK*), 1% L-Glutamine (*Gibco Glutamax™, South America*) and 1% Penicillin-Streptomycin antibiotics.

In order to culture Primary *HUVEC* unpassaged cells; 10 cm^2 polysterene culture dishes (*Nunclon™, USA*) were first treated with the mixture of fibronectin (*Sigma-Aldrich, USA*) and gelatin (*Dr Oetker, UK*). Fibronectin and gelatin coated dishes were dried at 37°C. Excess solution was removed after 45 min and the plates were dried for 20 additional minutes in sterile conditions. These treated plates were then cultured with primary *HUVEC* cells in DMEM.

3.2 Cell lysate Preparation:

All the cells were cultured in 10 cm^2 cell culture dishes at 2×10^6 cell density overnight. Cultures were removed of any traces of media and washed four times with 500 mM HEPES and 137 mM NaCl buffer (Wash Buffer). These cells were collected with cell scraper (*Greiner, Sigma-Aldrich, USA*) in 1 ml wash buffer and freeze-thawed three times. Freezing was done at -20°C while thawing at +37°C. Cells were disrupted under the pressure of 23 Gauze needle (*BD Plastipak, Spain*). Proper cell lysis was confirmed by microscopy using Light Microscope (*Olympus CKX31*) at 20X magnification.

3.3 Bradford Assay:

The protein content of the cell lysates was measured using the Bradford Assay's (*BioRad Protein Assay, USA*). Bovine Serum Albumin *(Sigma-Aldrich, USA)*, 1 mg/ml was used as a standard solution. All dilutions were made in distilled H_2O to avoid phosphate interference. The standard curve equation was used for assessing protein content in unknown samples.

Samples and controls were in 800 μl volume, and 200 μl BioRad solution was added to them (Table A4). After 5 min of incubation for color development, the absorbance was measured at 590 nm using Spectrophotometer (*Victor™ XM4 2030 Multilabel Reader, Perkin Elmer, USA*) (Fig. 6).

3.4 Pyrophosphate Measurement:

3.4.1 PPi evaluation with commercial Kits:

The available contemporary methods three commercial kits, i.e. PiPer™ Pyrophosphate Assay Kit (*Life Technologies*), Pyrophosphate Assay Kit, Fluorometric (*ab112155,*

Abcam) and PPiLight™ Inorganic Pyrophosphate Assay (*Lonza*), were used for comparing PPi calculated with $ZnCl_2L$ probe. All the kits were executed according to their manufacturers protocols.

PiPer™ Pyrophosphate Assay Kit (*Life Technologies*)

In PIPER kit (*PiPer™ Pyrophosphate Assay Kit, Life Technologies, USA*), inorganic pyrophosphatases are used to break down available PPi in the sample to two equivalents of inorganic pyrophosphate (Pi). Proceeding further, maltose phosphorylase converts glucose-1-phosphate to glucose in the presence of Pi. Glucose oxidase turns glucose to gluconolactone and hydrogen peroxide (H_2O_2). Utilizing Horseradish peroxide (HRP) H_2O_2 reacts with Amplex Red Reagent (10-acetyl-3,7-dihydrophenoxazine), which gave the fluorescent, compound Resorufin. Resorufin has emission maxima at 587 nm when excited at 563 nm (Fig. 3).

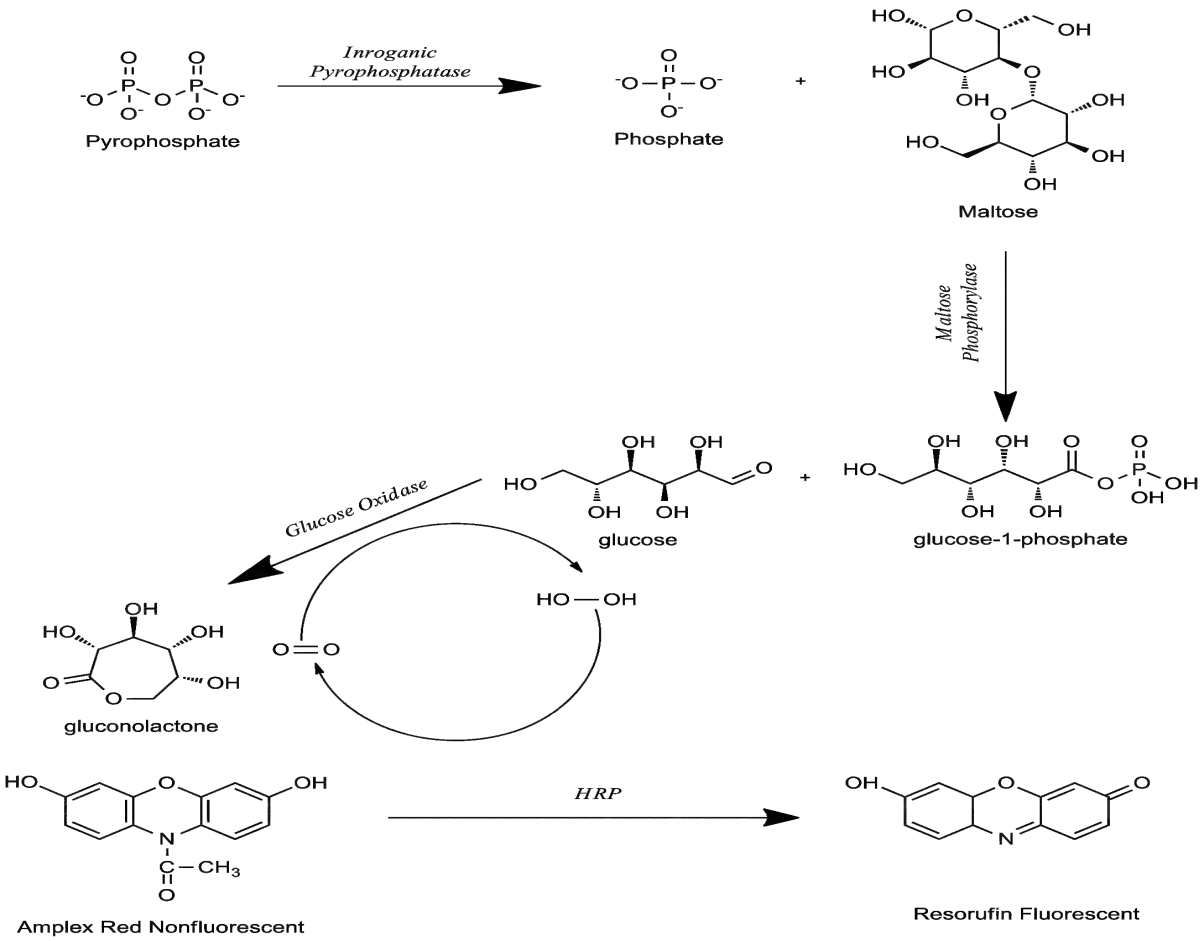

Fig. 3 Demonstration of PiPER Kit Cascade reaction process. Pyrophosphatte (PPi) molecules are first broken down into Inorganic Phosphate (Pi). Maltose in the presence of maltose phosphorylase breaks Pi into glucose-1-phosphate and glucose, which is further converted in gluconolactone and H_2O_2 by glucose oxidase. Amplex Red Reagent using HRP as catalyst converts H_2O_2 in the final step to the fluorescent Resorufin (Image based on: https://tools.lifetechnologies.com/content/sfs/manuals/mp22062.pdf)

The first step of this cascade reaction generates Pi, which is exploited in downstream steps for PPi detection. This raised a question whether the final amount of pyrophosphate detected by the kit is selectively the PPi amount or does it encompass all the available inorganic phosphate (Fig. 5).

Stock solutions were prepared as directed in the instructions (*Molecular Probes*^{TM} *Invitrogen MP22062*). Cell lysates equivalent to 100 μg protein were diluted in 1X reaction buffer (500 mM Tris-HCl, 5 mM $MgCl_2$, pH 7.5) to attain the final volume of 50 μl. These along with PPi standards and controls were pipetted in 96-well plates (*Isoplate Tm-96F, Perkin-Elmer, USA*) (Table A1). The reactions were initiated by adding 50 μl of PIPER solution (composed of 100 μM Amplex Red reagent containing 0.02 U/ml

inorganic pyrophosphatase, 4 U/ml maltose phopshorylase, 0.4 mM Maltose, 2 U/ml glucose oxidase, 0.4 U/ml HRP) (Table A2). The plate was incubated in dark at 37°C for 30 min before the fluorescence was recorded. Excitation and emission filter of 485 nm and 579 nm respectively (*Victor^{TM} XM4 2030 Multilabel Reader, Perkin Elmer, USA*) were used. PIPER solution was used within 15 min of composition and was made fresh each time the measurements were done.

Pyrophosphate Assay Kit, Fluorometric (*Abcam*)

Abcam (*ab112155, Abcam, UK*) kit relies on the use of light-sensitive fluorogenic photosensitive sensor. This is possibly the closest method to the $ZnCl_2L$ probe's protocol can be compared with. Pyrophosphate standards and cell lysates were prepared from stock as mentioned in the kit's instructions to a final volume of 50 μl (Ref). All the samples along with 50 μl of assay solution provided in the kit were pipetted in the 96–well plates and incubated for 30 min at RT before assessing the fluorescence with excitation at 340 nm ±25 nm and emission at 460 nm (*Victor^{TM} XM4 2030 Multilabel Reader, Perkin Elmer, USA*).

PPiLight^{TM} Inorganic Pyrophosphate Assay (*Lonza*)

In Lonza kit (*PPiLight^{TM} Pyrophosphate Detection Kit, LT07-610, Lonza, Switzerland*), PPi is investigated by the amount of light produced by Luciferase on conversion of AMP to ATP using available PPi in test sample (Fig. 4).

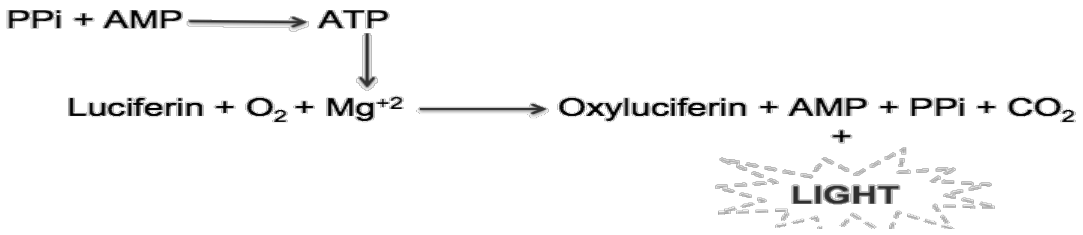

Fig. 4 Presentation of the PPi detection mechanism by PPiLight^{TM} Inorganic Pyrophosphate Assay (*Lonza*) commercial kit. Image based on PPiLight^{TM} Inorganic Pyrophosphate Assay's (*Lonza*) Protocol

Pyrophosphate standard and control samples were prepared with the reconstitution buffer provided in the kit. Cell homogenates equivalent to 100 μg of protein content were

diluted in the reconstitution buffer to a final volume of 40 μl. 20 μl of PPiLight™ converting reagent and PPiLight™ detection reagent was added sequentially to the samples and were incubated for 30 min at RT after each addition. Luminescence was recorded with 0.1 s (integrated) read time.

3.4.2 PPi evaluation with $ZnCl_2L$ probe:

Cell lysates were diluted in 50 μM $ZnCl_2L$ probe in a quartz cuvette (*Hellma® Analytics, Germany*) in 1:100 ratio i.e. 20 μl of lysate in 2 ml of probe. Probe was allowed to stand for 3-5 min for complex formation before sample was excited at 440 nm through 5 nm slit width for each measurement at 37°C. Emission was recorded between 450-670 nm via 10 nm slit width. Fluorescence Spectrophotometer (*Varian Cary Eclipse, Agilent Technologies*) was used for probe-based measurements.

3.5 Time point measurements at 37°C:

Stability of the PPi measurements were checked by incubating cell homogenates at 37°C for four different time points i.e. 30 min, 60 min, 150 min and 24 hr. Fluorescence was measured with fluorescence spectrophotometer (*Varian Cary Eclipse, Agilent Technologies*) utilizing previously described settings (Section 3.4.2).

3.6 Confocal Analysis:

To observe the fluorescent binding phenomena of the probe with cells confocal microscopy was used. Cells were cultured in 8–chambered glass plates (*Nunclon™, USA*) according to the conditions suitable for each type. Cells were washed with wash buffer and incubated with 50 μM $ZnCl_2L$ probe for 25 min at 37°C. Cells incubated with washing buffer alone for 25 min were used as control. Prior to imaging, cells were washed four times in wash buffer to remove traces of excess probe. Cells were excited at 488 nm wavelength and observed with 60X magnification objective. Olympus Microscope IX81 with Fluoview 1000 Confocal setup was used.

3.7 MTT Assay:

Cytotoxic effect of the probe on live cells was evaluated using MTT (3-[4,5-Dimethylthiazol-2-yl]-2,5-diphenyltetrazolium bromide) Assay. *HeLa-MZ* cells at density of 4000 cells/well were grown in 96–well plate. Media was discarded and cells were incubated with 50 μM $ZnCl_2L$ probe in 500 mM HEPES and 137 mM NaCl buffer for 30 min, 60 min, 150 min and 24 hr at 37°C. MTT solution was prepared by dissolving 0.5 mg/ml of MTT powder (*Sigma-Aldrich, USA*) in phenol free media. Probe was removed and 100 μl of MTT solution was added to the wells at 37°C. After three hours, 100 μl of lysis buffer was added (0.04 N HCl in Isopropanol) to dissolve formazan crystals formed by reduction of MTT in metabolically active cells. All the steps were done in light protected conditions. Plates were re-incubated at 37°C for one hour and read at 570 nm wavelength with Microplate reader (*Victor^{TM} XM4 2030 Multilabel Reader, Perkin Elmer, USA*).

Formula used to analyze the percentage of cell viability was as follows:

$$\%\ cell\ viability = \left({}^{test\ cells}/_{ctrl\ cells}\right)\times 100 \quad \ldots(1)$$

Test Cells: Cells incubated with probe

Ctrl Cells: Cells incubated with media

3.8 Statistical Analysis:

Samples were compared statistically with *t*-test using Prism software. Since the data concerning percentage values was not normally distributed, arcsine square root transformation of the original variable was done to obtain a normal distribution of the binomially distributed data. Otherwise, parametric test might have rendered misleading results.

4. Results:

4.1 PPi evaluation with $ZnCl_2L$ probe *vs.* commercial kits:

To measure the PPi content in cell homogenates different types of cells were used. Some of them were non cancerous such as *GMK, MF, RF, HUVEC* and others were cancerous such as *MDA MB 231, A549, HeLa-MZ, HEP G2*. The PPi levels were evaluated using different kits and the probe for the analysis. Purified PPi was used to prepare a standard for comparing the different measurement protocols, and for evaluating the PPi levels in the homogenates (Fig. 5). The kits had varied levels of sensitivity towards PPi. The PIPER kit was most responsive for PPi concentrations between 10-40 μM. The regression factor of 0.89 (Fig. 5A) was acquired from this range whereas when tested with 2-10 μM it depreciated to 0.26 suggesting that the PIPER kit was not able to detect concentrations below 10 μM PPi efficiently (Fig. 11C). Abcam kit had no sensitivity towards PPi in the tested micro molar range (Fig. 5D). Recommended concentrations from 0-10 μM in the Abcam's protocol for the standard curve resulted in random fluorescence intensities instead of expected linear increase (Fig. 5D). On the other hand, the Lonza kit detected concentrations even in sub micro molar range from 0-1 μM with a regression factor of 0.93 (Fig. 5C). Regression factor elevated to 0.96 when the concentration was increased to 1-10 μM with the Lonza kit. On a completely different note, the fluorescence data obtained with the $ZnCl_2L$ probe generated the regression factor of 1.0 when plotted (Fig. 5B).

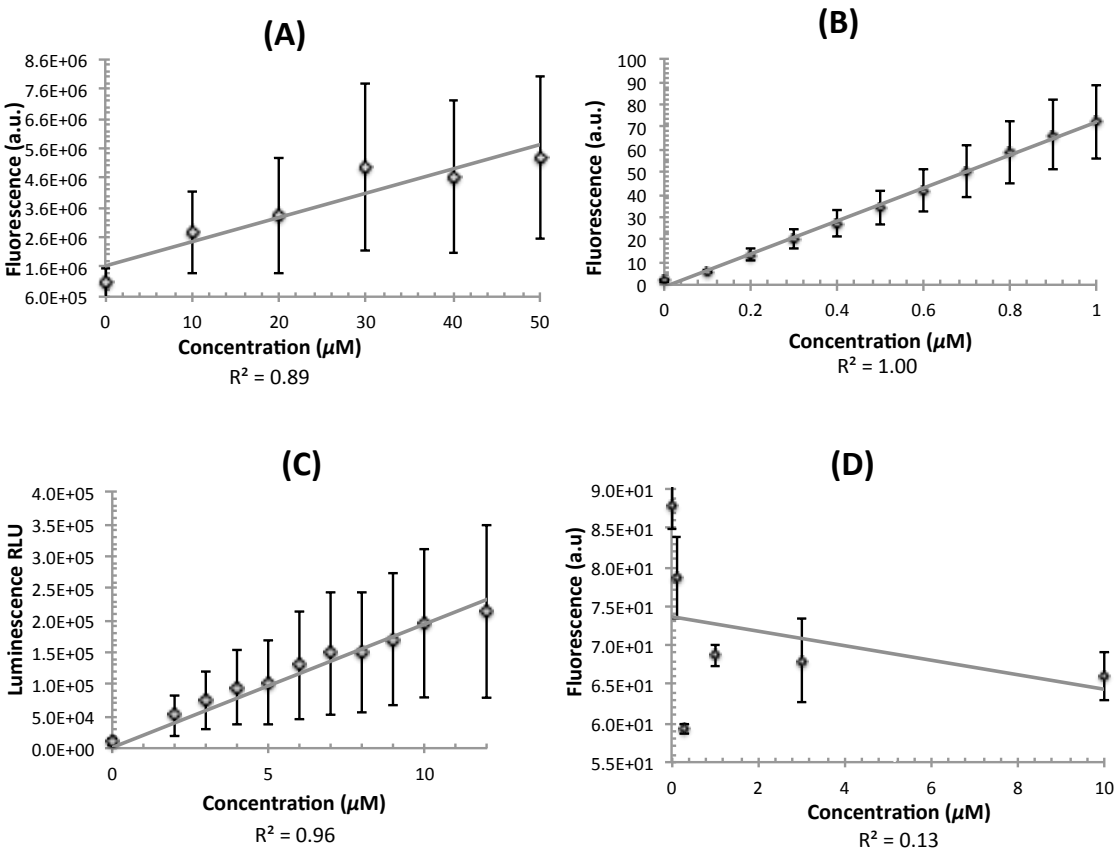

Fig. 5 Fluorescence and luminescence values obtained from pure PPi concentration when investigated with commercial kits (A) PiPer^{TM} Pyrophosphate Assay Kit (*Life Technologies*), (B) 50 μM $ZnCl_2L$ probe, (C) PPiLight^{TM} Inorganic Pyrophosphate Assay (*Lonza*) and (D) Pyrophosphate Assay Kit, Fluorometric (*ab112155, Abcam*). Concentrations of (A) 0-50 μM, (B) 0-1 μM, (C) 0-12 μM and (D) 0-10 μM were tested according to their sensitivity range. The values given here are the mean representation of three repeats performed (±Std Error).

The cell homogenate values were calculated based on the linear regression equation acquired from the PPi curve from each method. Surprisingly, it was found that the cell sample values resulting from the measurements with the Lonza and Abcam kits had lower values than the blank samples, which consisted only buffer. Therefore reliable quantification of homogenate values with either Lonza or Abcam kit was not possible (Fig. A3). In addition to that, the Abcam kit had no response to micro molar PPi concentrations, therefore no regression equation was obtained (Fig. 5D). As a result, PPi could not be analyzed with the Abcam kit.

Despite of the low sensitivity towards PPi demonstrated by PIPER kit, both of the conditions required for quantitating pyrophosphate concentration were met (Table 3). First of the two conditions were to have a valid regression equation and second that the

fluorescence values in test samples must exceed blank values. Concentrations analyzed by the PIPER kit were more than thousands of folds higher for the homogenates compared to those obtained from the probe (Table 3).

Table 3 PPi content in μmol/ 100 μg protein units when investigated with commercial kits (PiPer^{TM} Pyrophosphate Assay Kit (*Life Technologies*) and 50 μM $ZnCl_2L$ probe. The values given here are the mean values of three repeats performed (±Std Error). PPi content assessed by the PIPER kit was multiple folds higher from 50 μM $Zncl_2L$

Sample type	**PPi (μmol) with $ZnCl_2L$ Probe /100 μg protein**	**PPi (μmol) with PIPER /100 μg protein**
MDA MB 231	5.8±2.7	$1.8 \times 10^3 \pm 1.1 \times 10^3$
HEP G2	4.6±2.9	$7.8 \times 10^3 \pm 4.2 \times 10^3$
HeLa-MZ	6.8±2.6	$6.4 \times 10^3 \pm 4.2 \times 10^3$
A549	5.2±1.5	$4.6 \times 10^3 \pm 2.8 \times 10^3$
GMK	4.4±1.9	$3.1 \times 10^2 \pm 2.1 \times 10^2$
MF	4.2±1.6	$1.1 \times 10^4 \pm 6.6 \times 10^3$
RF	4.1±1.2	$3.3 \times 10^3 \pm 1.8 \times 10^3$
Pr HUVEC	2.2±1.0	$6.9 \times 10^2 \pm 8.2 \times 10^2$
HUVEC	3.0±1.2	$3.3 \times 10^4 \pm 1.4 \times 10^4$

In the experiment done on different days variations were observed in the obtained fluorescence values. The PPi concentrations obtained from both the experiments were normalized and used to test the statistical significance (Fig. 6, 7). When using the probe, variations between untransformed *MF, RF, Pr HUVEC, HUVEC* and transformed *HeLa-MZ* were statistically significant with $p<0.001$ (Fig. 6). Cancerous cell types *A549* and *HEP G2* were statistically insignificant with *p*-values 0.07 and 0.05 respectively when tested against *HeLa-MZ.* The *t*-test was performed in reference to *HUVEC* cells in case of the PIPER kit (Fig. 7). The untransformed *Pr HUVEC, GMK, MF, RF* along with transformed *HEP G2, HeLa-MZ, A549* cell types possessed varying degree of variation from the reference. Surprising fact was that the PPi content was 100-fold higher from *Pr HUVEC* and *GMK*, which belong to the same untransformed series of cells as *HUVEC* itself.

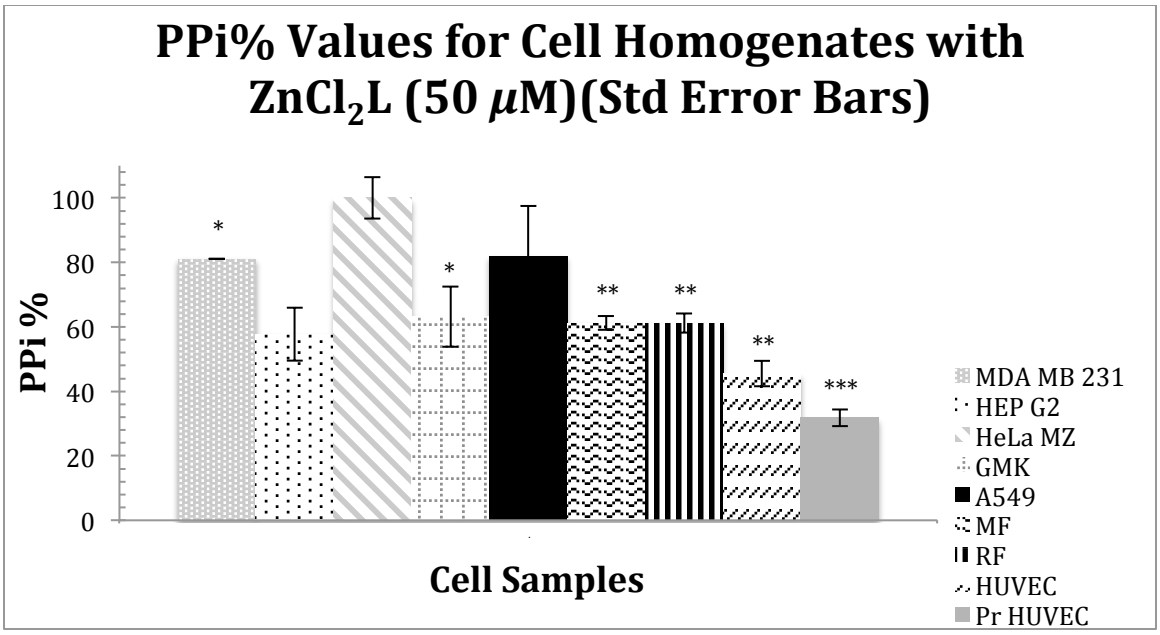

Fig. 6 Graph portraying PPi percentage in series of cell homogenates evaluated using 50 μM $Zncl_2L$ probe. The concentrations of PPI were first normalized to 100 μg of protein. Then the highest PPi value of Hela cells was taken as a reference for easier comparison of PPi values of different cell types. Assay was repeated three times (±Std Error). Statistical significance was tested with Student's *t* test (***p< 0.001, **p<0.001, *p<0.05) between *HeLa- MZ* and other cell types.

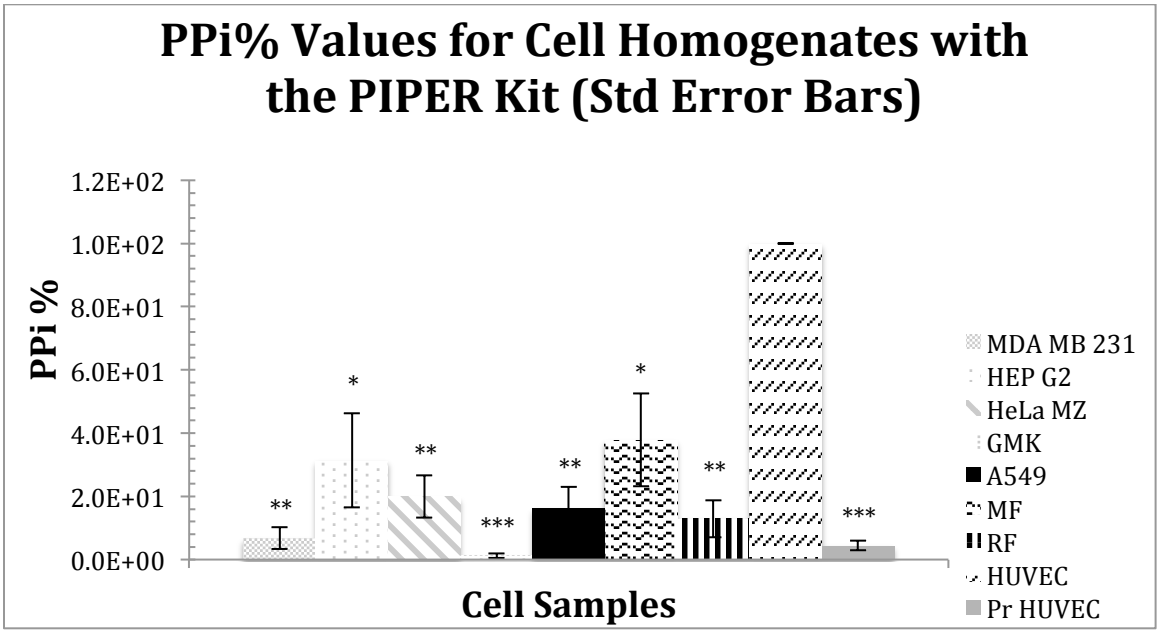

Fig. 7 Graph portraying PPi percentage in series of cell homogenates evaluated using PiPer™ Pyrophosphate Assay Kit (*Life Technologies)*. The concentrations presented here were first normalized to 100 μg of protein as in Fig. 6. The highest PPi value of Huvec cells was taken as a reference to measure the PPi% values for all cell types. Assay was done three times (±Std Error). Statistical significance was tested with Student's *t* test (***p< 0.001, **p<0.001, *p<0.05) between *HUVEC* and other cell types.

4.2 Stability of the 50 μM $ZnCl_2L$ probe-PPi complex at different time points:

As there was no preliminary information on whether the PPi measurements with the samples would be stable over time with the probe, stability over the period of 24 h with two cell types, GMK and HeLa-MZ cells. The measurements done on *GMK* and *HeLa-MZ* cells were found to be quite stable (Fig. 8). The PPi content remained static in both cell types for the monitored period with only minor fluctuations. *GMK*s had PPi levels of 2.3±0.7 μmol/ 100 μg protein at 30 min, with insignificant loss of 0.4 μmol by 24 hr. The PPi concentration in *HeLa-MZ* was reduced by 0.5 μmol from 30 min to 3.9±1.2 μmol/ 100 μg protein at 24 hr. The differences between the time points were not statistically significant (p>0.05) in both cell types. When tested in reference to the 30 min time point values p-values for *GMK* were 0.08, 0.43 and 0.21 for 60 min, 150 min and 24 hr time points, respectively. In case of *HeLa-MZ* cells p-values of 0.10 and 0.18 were obtained for 60 and 150 min with a variation of **p<0.001 at 24 hr time point (Fig. 8).

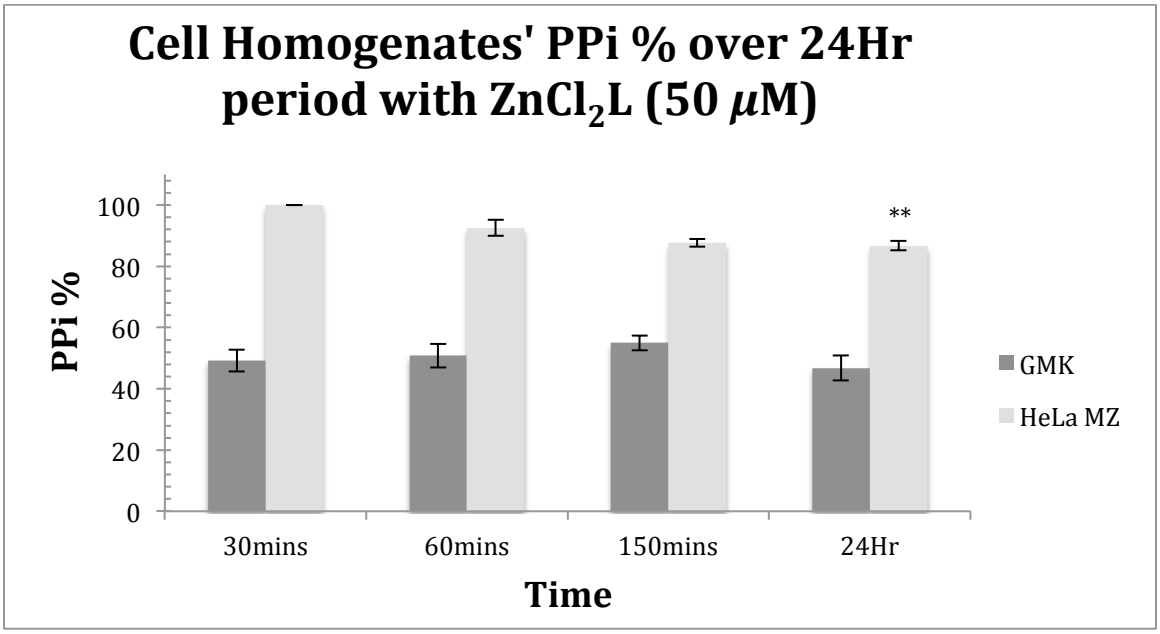

Fig. 8 PPi content measured with $ZnCl_2L$ probe in *GMK* and *HeLa-MZ* cell lines after incubation at 37°C for 30 min, 60 min, 150 min and 24 hr. Concentrations were first normalized to 100 μg protein and then compare in ratio to the highest value of *HeLa-MZ* cells at 30 min time point for easier comparison. Values represented here are the mean of three repeats (±Std Error). Statistical significance was tested with Student's t test (**p<0.001) in reference to 30 min time point of both cell lines.

The PPi values measured with the PIPER Kit declined drastically over the duration of 90 min. The amounts reduced by a factor of 31.4±8.5 in 90 min (Fig. 9). However, as there

was huge variation in the result of the three repeats, the differences were not statistically significant, except for *GMK* cells during 60 min time point. The *p*-values for *HeLa-MZ* were 0.87 and 0.18 for 60 min and 90 min respectively when tested in reference to 30 min. One-tailed test showed **$p<0.001$ significance at 90 min for *HeLa-MZ* cell type (Fig. 9).

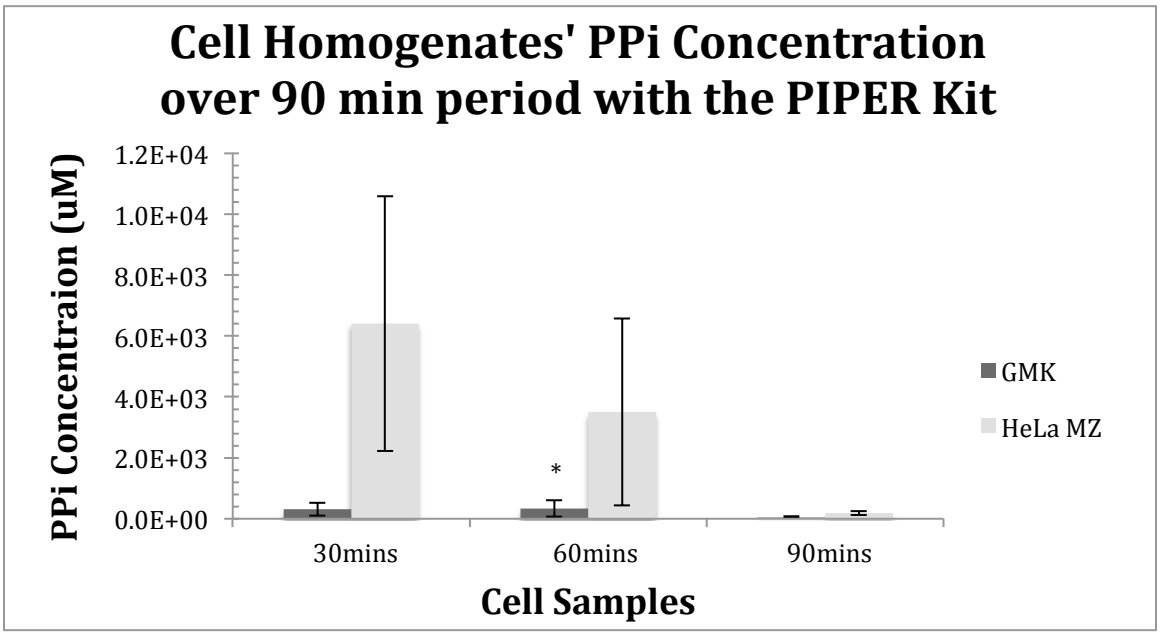

Fig. 9 PPi content measured with PIPER Kit in *GMK* and *HeLa-MZ* cell lysates for 30 min, 60 min and 90 min time-points at 37°C. Concentrations were normalized to 100 μg protein. Assay was replicated three times (±Std Error). Statistical significance was tested with Student's *t* test (*$p<0.05$) in reference to 30 min time point.

With the Lonza kit the measured values were expected to increase over time. When PPi concentrations below 1 μM were tested fluorescence values didn't increase. However, regression remained stable over 90 min at PPi concentrations above 1 μM (Fig. 10), therefore, demonstrating lack of sensitivity in the sub-micromolar range.

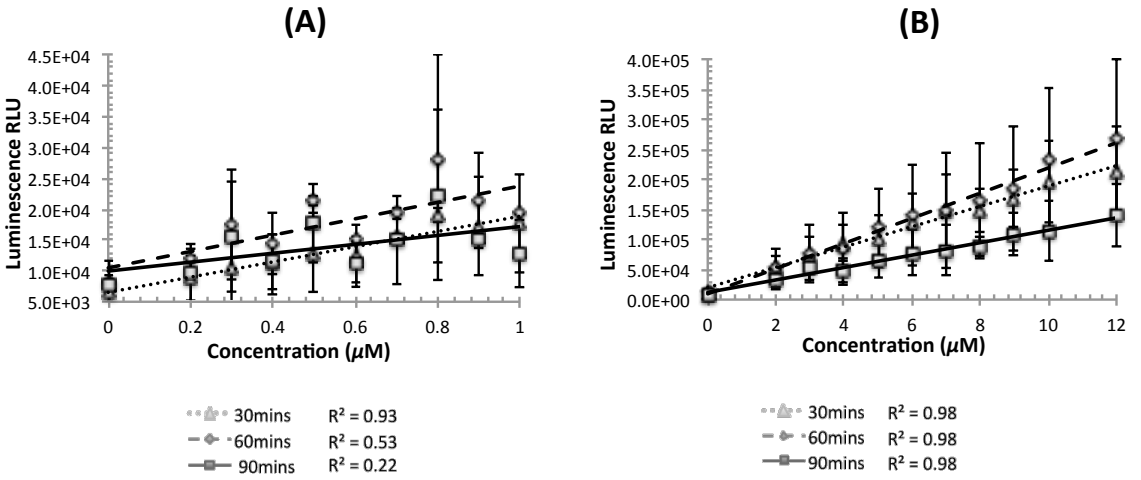

Fig. 10 Known PPi amounts in (A) 0-1 μM (B) 0-12 μM concentrations measured with PPiLight™ Inorganic Pyrophosphate Assay (*Lonza*) Kit at 30 min, 60 min and 90 min time-points. (A) Depreciation in the intensity was noted in concentrations over 60 min duration. The regression however remained static over 90 min duration at higher concentrations (B). Values represented are mean of three repeats (±Std Error).

4.3 Inorganic Phosphate (Pi) measurement with PiPer™ Pyrophosphate Assay Kit (*Life Technologies*):

As there was a concern that the PIPER kit measuring Pi in addition to PPi in the homogenates and would contribute significantly to the results, the sensitivity of the kit to Pi was tested. The kit efficiently detected concentrations below 40 μM of Na_3PO_4. It represented regression factor of 0.97 and 0.94 for 0-10 μM & 0-40 μM concentrations respectively. The kit has higher sensitivity for Pi than for PPi concentration range of 0-40 μM. (Fig. 11). This may explain the exceptionally high values of PPi calculated from the kit compared to the probe's assessment of homogenates (Fig. 9).

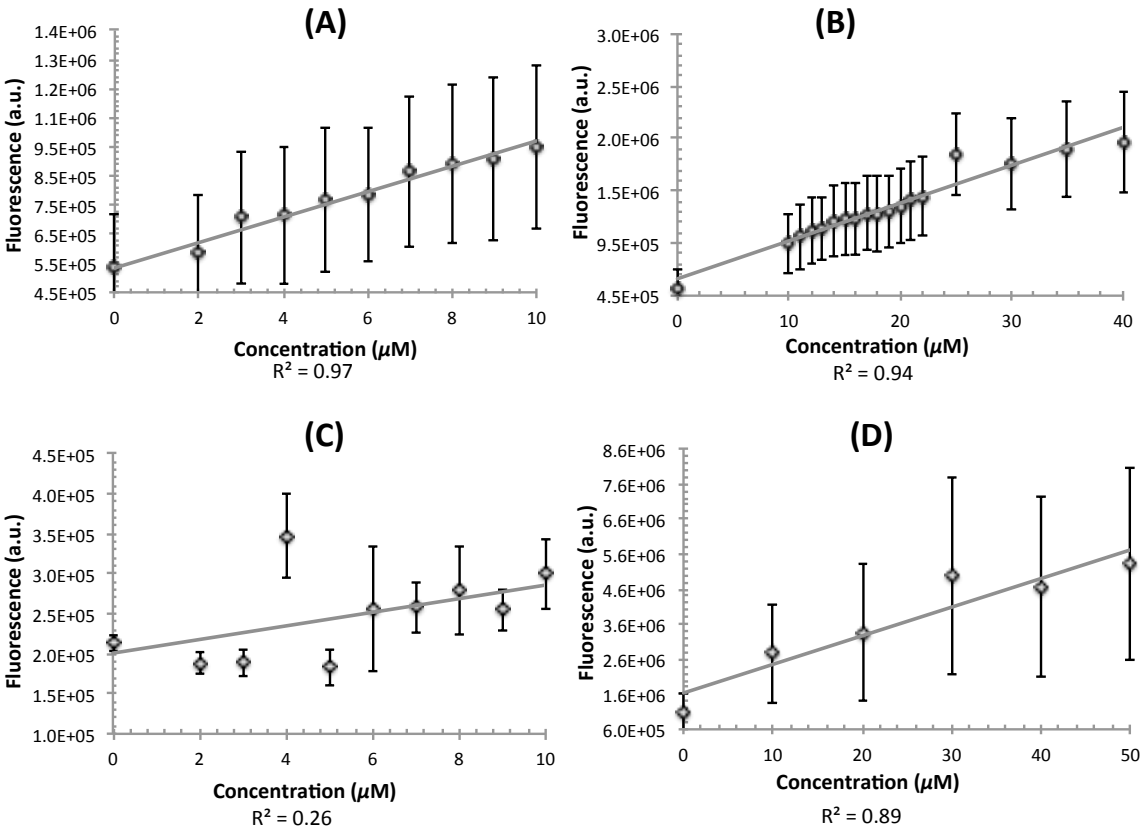

Fig. 11 PIPER Kit was tested towards its sensitivity towards Na_3PO_4.When such samples were detected with the PiPer^{TM} Pyrophosphate Assay Kit (*Life Technologies*) they rendered regression factor of (A) 0.97 for 0-10 μM & (B) 0.94 for 0-40 μM of Na_3PO_4 after 30 min incubation at 37°C in 96-well plates. Comparatively, graphs generated by using known concentrations of PPi (C) 0-10 μM (D) 0-50 μM from the kit yielded lower regression factors of 0.26 and 0.89 respectively than for phosphate measurements.

4.4 Stained *vs* Unstained Cells with $ZnCl_2L$ probe under Confocal setup:

With the help of Olympus confocal setup stained and unstained cells were excited and analyzed at excitation of 488 nm. The cells, which were incubated with the $ZnCl_2L$ probe appeared bright orange in color in the cytoplasm whereas the control cells appeared mostly dark in the fluorescent channel (Fig. 12). Rare fluorescent dots appeared in some control wells, which were most probably due to the auto-fluorescence of the rounding up and detaching cells over extended periods of observation. The images were gathered from the confocal microscope and using ImageJ software.

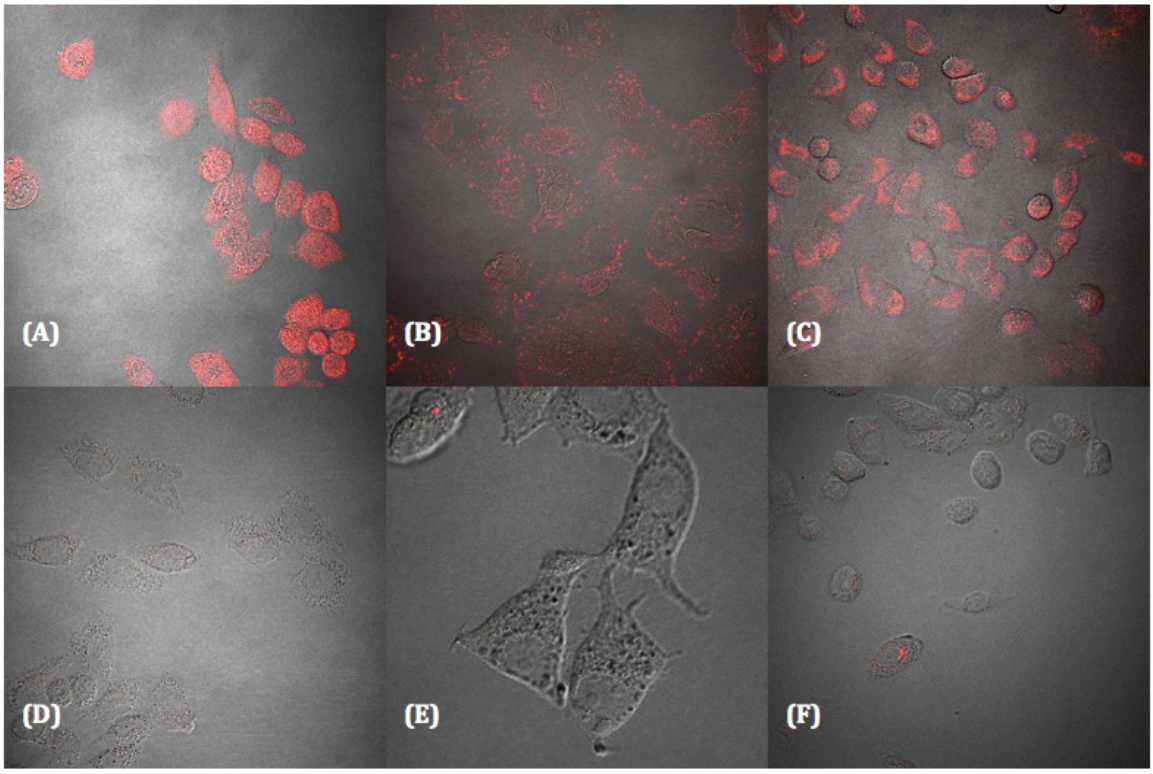

Fig. 12 Overlaid DIC & Fluorescent channel confocal fluorescence microscopy images of (A) *Hela-MZ*, (B) *GMK* and (C) *A549* cells incubated for 25 min at 37°C with 50 μM $ZnCl_2L$ probe in wash buffer and imaged (at 60X magnification); Controls (D) *Hela-MZ*, (E) *GMK* & (F) *A549* without the probe were incubated in 500 mM HEPES and 137 mM NaCl Buffer for 25 min at 37°C

4.5 Cytotoxic Effect of $ZnCl_2L$ probe on *HeLa-MZ*:

The cytotoxic impact of the probe on the cells was examined with the help of MTT assay. Cells without the probe were used as control. Cell viability was followed for a 24 hr period. Viability of over 80% after 30 min suggested the measurements within this limit are still acceptable (Fig. 13). A depreciation of more than 15% in the cell viability was observed already at 150 min time point suggesting that the probe or the buffer conditions are affecting the cell viability already in a couple of hours.

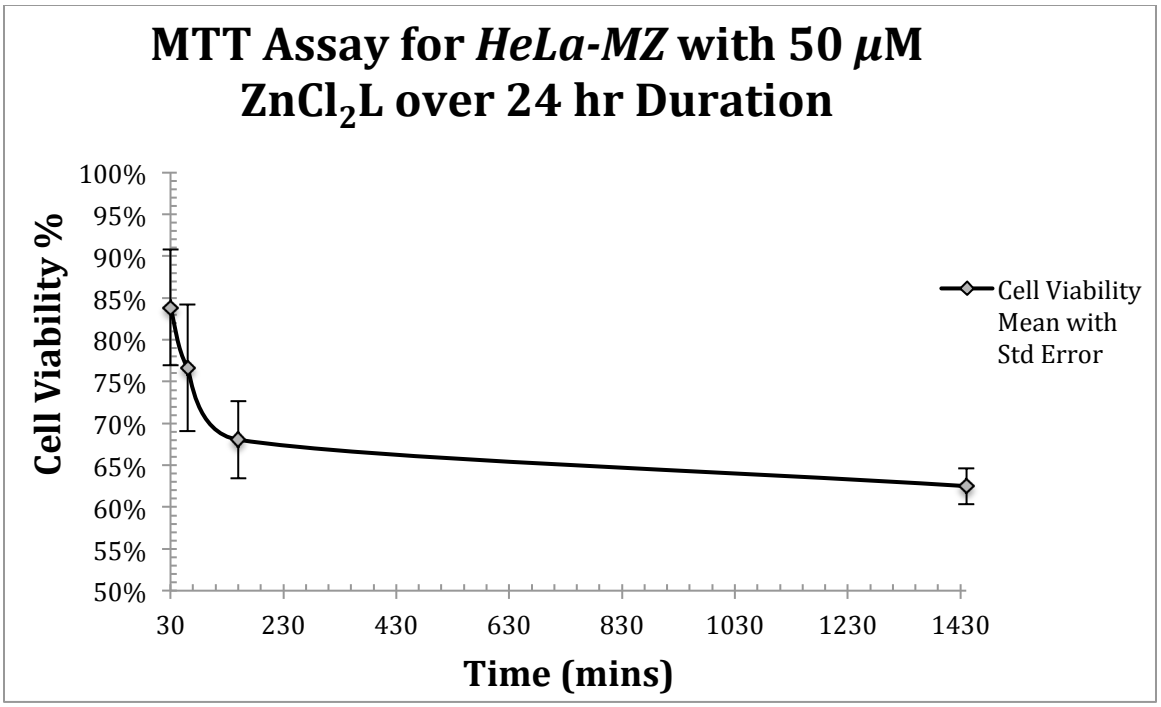

Fig. 13 Toxicity of 50 μM $ZnCl_2L$ probe on *HeLa-MZ* cells represented graphically. MTT assay was performed on cells and were incubated for 30 min, 60 min, 150 min and 24 hr at 37°C. Percentage of viable cells were calculated with the formula (1). The values are mean obtained from three repetitions performed (±Std Error). Viability dropped from 83.8% at 30 min time point to 62.5% after 24 hr incubation with the probe. 100% viability was calculated with the cells without the probe.

5. Discussion:

The experiments conducted as a part of my work contributed to the search for accurate PPi measurement of pure PPi preparations as well as in cellular samples. To assess the probe's performance over other available techniques three commercial PPi measuring kits were implemented. At first, 0-1 μM PPi concentrations were used to generate similar scaled standard curves for kits and the probe. As the PIPER kit was unable to measure 0-1 μM PPi concentrations, higher concentrations varying from 0-50 μM were used instead (Fig. 5, 11). Lonza's detection of pure PPi samples in 0-1 μM PPi range provided a good response curve instead. In contrast to Lonza's measurements, Abcam was not able to detect PPi standard samples in micro molar range. The kit responded only to milimolar quantities. Such low sensitivity would be futile to measure cell based PPi values, which are more in the micro molar scale. The luminescence-based Lonza kit had detected pure pyrophosphate samples unambiguously (Fig. 5C).

While optimizing the standard curve for the Lonza kit 0-12 μM PPi range was chosen for cell PPi measurements. However, the kit demonstrated lower luminescence for cell homogenates than for the blank samples in the standard curve measurement. Upon achieving unexpected cell lysate values with respect to blank another standard curve with lower PPi values (0-1 μM) was run in parallel with the cell lysates. The standard curve advanced in approximately linear fashion whereas the cell samples still had lower luminescence than the lowest standard curve values. Reflecting back on the principle reaction of Lonza kit (Fig. 4), the unexpected results may have something to do with the cellular status of ATP, which is measured in the kit. The experiments were performed three times and the pattern was found consistent. Moreover, chances of contamination by PPi in the wash buffer was not possible as the same buffer was used for both the Lonza kit and probe.

The PIPER kit resulted in PPi values over 100 times higher in the homogenates than that measured by the $ZnCl_2L$ probe (Table 3). The variations between the measured content by the kit and probe were enormous. This led to suggestion that perhaps the phosphate contents in the homogenates was increasing the PIPER result and not the PPi. Therefore, further analysis of the assessed values using trisodium phosphate (Na_3PO_4) as a source for inorganic phosphate was used (0-40 μM). As PIPER kit very efficiently and

sensitively measured the phosphate, it is thus possible that high cellular phosphate values are contributing to the PIPER PPi measurement results.

Quite varying results have been received from tissue and cell culture measurements (Table 3). According to the $ZnCl_2L$ probe based measurements the highest PPi was in the range of 5-7 μmol per 100 μg of protein content in cancerous *HeLa-MZ, MDA MB 231* etc. cells. Lowest values of 2.2 μmol per 100 μg protein were in primary *HUVEC* cells (Table 3). On the other hand on manifold lower scale Lust *et al.* (1976) reported 322±66 pmol PPi in skin fibroblasts when plated at cell density of 1×10^6. McGuire *et al.* (1980) assessed approximately four times higher values by using different method on the same cell type. Terkeltaub *et al.* (1994) found 50pmol PPi/μg cell protein to be present in transformed simian fibroblasts. McGuire *et al.* (1980) got the concentrations of 845±344, and 387±86 pmol respectively per μg of DNA in bone cells and synovial cells. Lust and Seegmiller, (1976) had more than three times lower PPi concentration in chondrocytes compared to McGuire *et al.* (1980). Implementation of the same radioactive labeling method by Cheung and Suhadolnik (1977) depicted results varying in order of magnitudes in cultured human chondrocytes i.e. 62 nmol/μg protein and 457±60 pmol/µg DNA (McGuire *et al.,* 1980; Lotz *et al.,* 1995).

Peters *et al.* (1984) and Ryan *et al.* (1986) found while working on fibroblasts that multitude of factors such as variations in the age, harvesting technique, environment of cultured cells, number of passages, and extraction buffer used were influential in determining the PPi of a particular cell type. Previous researchers have evaluated the PPi values in reference to several factors such as DNA, protein or cell number. Based on Heinonen (2001)'s assumption of the presence of 5 pg DNA in each diploid cell the arithmetic estimations were made to establish common grounds for rough comparisons with literature values. With the limited available information on the past works it was only possible to convert values expressed in terms of DNA to their possible cell number values but not in case of protein based references (Table 4). Fortunately, literature based on protein content optimization could be compared directly with the thesis work as they were also normalized in reference to protein (Table 3).

Table 4 Comparison of PPi concentrations obtained by various researchers are normalized to the number of cells.The association to number of cells in rest of the datasets is based on Heinonen (2001)'s assumption of each diploid cell containing an average of 5 *pg* DNA. These concentrations are theoretically obtained and do not represent accurate amounts rather provide an overview to compare the results.

Sample type	**PPi Concentration**
Skin Fibroblasts (Lust *et al.,* 1976)	322±66 *pmol*/10^6*cells*
Human Chondrocalcinotic Fibroblasts (McGuire *et al.,*1980)	1250±10 *pmol*/10^6*cells*
Normal Fibroblasts (Lust *et al.,* 1981)	270±70 *pmol*/10^6*cells*
Chondrocalcinotic Fibroblasts (Lust *et al.,* 1981)	400±80 *pmol*/10^6*cells*
Simian Fibroblasts (Terkeltaub *et al.,* 1994)	5 *nmol*/100μg *protein*
Chondrocytes (Lust and Seegmiller 1976)	655±46 *pmol*/10^6*cells*
Chondrocytes (McGuire *et al.,* 1980)	2285±300 *pmol*/10^6*cells*
Human Chondrocytes (Lotz *et al.,* 1995)	6.2 *nmol*/100μg *protein*

Table 5 PPi concentrations obtained are normalized to the number of cells. The concentrations of the cell lines in evaluations here were originally calculated in reference to the protein content (Table 3). For comparing, the obtained PPi amounts were manipulated based on the seeding density of the cell lines. These concentrations are theoretically obtained and do not represent accurate amounts rather provide an overview to compare the results with previous literature (Table 4).

Sample type	**PPi (μmol) with *$ZnCl_2$L Probe* /10^6*Cells***
MDA-MB-231	291.7±135.3
HEP-G2	233.8±145.8
HeLa-MZ	340.7±131.6
A549	263.2±77.8
GMK	224.4±96.1
MF	211.5±84.9
RF	207.0±64.9
Pr HUVEC	114.1±51.6
HUVEC	154.3±61.3

Despite the difficulties in directly comparing the literature values to the values obtained in this thesis, it was clearly seen that the probe resulted in the order of magnitude difference to the literature calculations.

To ensure the credibility of sensor-based data, interference from the probable compounds was tested. Rissanen's group noticed that the probe's efficiency was perturbed significantly in the presence of ATP, ADP and Pi when present in excessively high

concentrations. These interfering compounds could have significant impact if only supervened over 0.001 equivalents of PPi by 1 equivalent of the interfering anion (Bhowmik *et al.,* 2014). Sarpel *et al.* (1982) have demonstrated ATP to be in the range of 1.6±0.7 μmol/ml of erythrocytes, which does not supersede the tolerance threshold of the probe i.e. 13.3 μM for 50 μM working solution of the probe. Therefore, it is unlikely that interference would be due to the presence of ATP, ADP in the lysates. However, in the future experiments, the interference from ATP, GTP, phosphate or other probable molecules should be checked by adding excess amounts of the said compounds to homogenates.

In addition to these molecules, there are still several components in high amounts in the cells and extracellular samples. In order to acquire reliable measurements of PPi with the probe, careful precipitation of other organic molecules, preferably, one by one, needs to be done, in order to make sure no other substances are contributing to the measured values in complex samples.

Stability of the measurements plays an important role in analyzing the content. To comprehend the stability of PPi Ryan *et al.* (1986) extracted cells from osteoarthritic patients and evaluated pyrophosphate content both at the time of harvesting and six weeks later from the day. There was a considerable two-fold depreciation in the values of patients with the affliction (Ryan *et al.,* 1986). Protocol used was similar to the one in earlier mentioned studies revealing fluctuating values by McGuire *et al.* (1890) and Lotz *et al.* (1995). When the probe was used on the samples incubated over 24 hr time points no significant change in the content was observed.

Stability of the measurements with the kits were also explored over 90 min duration. It was especially emphasized in the Lonza kit's protocol that the readings increase for every concentration over a period of 60 min. However, when tested the trend followed for the standard PPi decreased instead of increasing (Fig. 10). The calculated values from PIPER kit declined rapidly as well.

MTT assay ascertained the viability of cells in probe to be over 80% at 25 min time point. It decreased by ~20% after 24 hrs of incubation with 50 μM probe at 37°C (Fig. 13). These values serve to be of relevance in qualitative analysis using Confocal Microscope

and live cell measurements (Fig. 12). Given the slight cytotoxicity of probe, live measurements should be executed within 30 min.

In a nutshell the probe serves as an easy, quick, efficient and ultra-sensitive sensor of PPi in pure preparations. It remains to be seen if the cellular measurements are faithful representation of the PPi content or if some other cellular substances are contributing to the values. The stable nature of the probe-PPi conjugate at room temperature and lack of light sensitivity makes it a very convenient tool in practice. In contrast, the available commercial kits have stringent requisites of temperature control and light sensitivity. Therefore, there is high hope for the probe usability in the future. However, extensive research needs to be done to prove its reliability.

6. Conclusions:

This project was focused on assessing the pyrophosphate content in the cells and ascertaining its accuracy. The main deductions of this thesis were:

1) Conduction of successful PPi determination by implementing 50 μM-working concentration of $ZnCl_2L$ probe diluted in HEPES Buffer.

2) The probe was remarkably stable at 37°C, and showed definitive PPi measurements varying harmoniously with different concentrations in contrast to commercial kits, i.e. *Life Technologies, Lonza* & *Abcam*. The probe was not sensitive to phosphate content in contrast to some commercial kits.

3) The probe showed higher values for highly carcinogenic cells lines (*HeLa-MZ, A549* etc.) in contrast to non-transformed cell types (*GMK, HUVEC* etc.).

4) The probe demonstrated concordant measurement of PPi content when subjected to test for both in vitro cell homogenates and under confocal microscope when imaged with live cells.

7. References:

Alfrey A.C., and C.C. Solomons. 1976. Bone pyrophosphate in uremia and its association with extraosseous calcification. *J.Clin.Invest.* 57:700-705.

Anzenbacher, P., M.A. Palacios, K. Jursiková, and M. Marquez. 2005. Simple electrooptical sensors for inorganic anions. *Org.Lett.* 7:5027-5030.

Armstrong, D., D. VanWormer, and C. C. Solomons. 1975. Increased inorganic serum pyrophosphate in serum and urine of patients with osteogenesis imperfecta. *Clin Chem*. 21:104-108.

Aw, T.Y., and D.P. Jones. 1985. ATP concentration gradients in cytosol of liver cells during hypoxia. *Am.J.Physiol.* 249:C385-92.

Beis I., and E.A. Newsholme.1975. The contents of adenine nucleotides, phosphagens and some glycolytic intermediates in resting muscles from vertebrates and invertebrates. *Biochem.J.* 152:23-32.

Berg, J.M., J.L. Tymoczko and Stryer L. 2002. Biochemistry. Aminoacyl-transfer RNA synthetases read the genetic code. New York: W H Freeman; Section 29.2. http://www.ncbi.nlm.nih.gov/books/NBK22356/

Bergman, T. 1967. Lecture to the royal swedish academy of science. *Torbern Bergman, Earth Scientist, Chymia.* 12:78.

Bhowmik, S., B.N. Ghosh, V. Marjomaki, and K. Rissanen. 2014. Nanomolar pyrophosphate detection in water and in a self-assembled hydrogel of a simple terpyridine-Zn2+ complex. *J.Am.Chem.Soc.* 136:5543-5546.

Caswell, A.M., M.K.B. McGuire, and R.G.G. Russell. 1983. Studies of pyrophosphate metabolism in relation to chondrocalcinosis. *Annals of the Rheumatic Diseases*, *42*(Suppl 1), 98–99

Caswell, A., D.F. Guilland-Cumming, P.R. Hearn, M.K.B. McGuire, R.G.G. Russell. 1983. Pathogenesis of chondrocalcinosis and pseudogout. Metabolism of inorganic pyrophosphate and production of calcium pyrophosphate dihydrate crystals. *Ann.Rheum.Dis*. 42:27-37.

Cheung C.P. and R.J. Suhadolnik. 1977. Analysis of inorganic pyrophosphate at the picomole level. *Anal Biochem.* 83:61-3.

Cong, Y.S., W.E. Wright, and J.W. Shay. 2002. Human telomerase and its regulation. *Microbiol.Mol.Biol.Rev.* 66:407-25.

Florence T.W.L. 2012. Genetics and mechanisms of crystal deposition in calcium pyrophosphate deposition disease. Curr Rheumatol Rep. 14:155–160

Guha, S., and S. Saha. 2010. Fluoride ion sensing by an anion interaction. *J.Am.Chem.Soc.* 132:17674-17677.

Goldwhite, H. 1981. Introduction to phosphorous chemistry, Cambridge University Press, Cambridge, England. 113pp.

Heinonen, J.K. 2001. Biological role of inorganic pyrophosphate, Kluwer Academic Publishers, Dordrecht, The Netherlands. 250pp.

Heimendahl M.V. 1981. Electron microscopy of materials: an introduction. Academic Press Limited, London. 228pp

Hirose, M., J. Abe-Hashimoto, K. Ogura, H. Tahara, T. Ide, and T. Yoshimura. 1997. A rapid, useful and quantitative method to measure telomerase activity by hybridization protection assay connected with a telomeric repeat amplification protocol. *J.Cancer Res.Clin.Oncol.* 123:337-344.

Hocking B.B.M. 2005. Handbook of chemical technology and pollution control. Academic Press, Elsevier, London. 830pp.

Johnson, . 1999.

Karasawa, K., Y. Sano, and H. Arakawa. 2014. Development of a novel telomerase assay using the PPDK-luciferin-luciferase detection system. *Luminescence.* 29:52-57.

Kim, J.H., J.H. Ahn, P.W. Barone, H. Jin, J. Zhang, D.A. Heller, and M.S. Strano. 2010. A luciferase/single-walled carbon nanotube conjugate for near-infrared fluorescent detection of cellular ATP. *Angew.Chem.Int.Ed Engl.* 49:1456-1459.

Klemme, J.H. 1976. Regulation of intracellular pyrophosphatase-activity and conservation of the phosphoanhydride-energy of inorganic pyrophosphate in microbial metabolism. *Z.Naturforsch.C.* 31:544-550.

Kukko, E., and J. Heinonen. 1982. The intracellular concentration of pyrophosphate in the batch culture of Escherichia coli. *Eur.J.Biochem.* 127:347-349.

Li, C., M. Numata, M. Takeuchi, and S. Shinkai. 2005. A sensitive colorimetric and fluorescent probe based on a polythiophene derivative for the detection of ATP. *Angew.Chem.Int.Ed Engl.* 44:6371-6374.

Lotz M., F. Rosen, G. McCabe, J. Quach, F. Blanco, J. Dudler, J. Solan, J. Goding, J.E. Seegmiller, and R. Terkeltaub .1995. Interleukin 1 beta suppresses transforming growth

factor-induced inorganic pyrophosphate (PPi) production and expression of the PPi-generating enzyme PC-1 in human chondrocytes. *Proc.Natl.Acad.Sci*. 24:10364-10368.

Lust, G., and J.E. Seegmiller. 1976. A rapid, enzymatic assay for measurement of inorganic pyrophosphate in biological samples. *ClinicaChimicaActa*. 66.241-249

Lust, G., G. Faure, P. Netter, A. Gaucher, and J. E. Seegmiller. 1981. Evidence of a generalized metabolic defect in patients with hereditary chondrocalcinosis. *Arthritis&Rheumatism*. 24:1517-1521

McGuire, M.B., C.H. Colman, N. Baghat, and R.G.G. Russell. 1980. Radiometric measurement of pyrophosphate in cell cultures. *Biochem.Soc.Trans.* 8:529-530.

Michael, A., J. Po, and G.H. Fallet. 1981. Measurement of soluble pyrophosphate in plasma and synovial fluid of patients with various rheumatic diseases. *Scand.J.Rheumatol.* 10:237-240.

Mikata, Y., A. Ugai, R. Ohnishi, and H. Konno. 2013. Quantitative fluorescent detection of pyrophosphate with quinoline-ligated dinuclear zinc complexes. *Inorg.Chem.* 52:10223-10225.

Pathak, R.K., K. Tabbasum, A. Rai, D. Panda, and C.P. Rao. 2012. Pyrophosphate sensing by a fluorescent Zn2+ bound triazole linked imino-thiophenyl conjugate of calix[4]arene in HEPES buffer medium: spectroscopy, microscopy, and cellular studies. *Anal.Chem.* 84:5117-5123.

Peters, G.J., E. Laurensse, A. Leyva, and H.M. Pinedo. 1984. Fluctuations in phosphoribosyl pyrophosphate levels in monolayer tumor cell lines. Effects of drugs. *FEBS Lett.* 170:277-280.

Quinlan, E., S.E. Matthews, and T. Gunnlaugsson. 2007. Colorimetric recognition of anions using preorganized tetra-amidourea derived calix[4]arene sensors. *J.Org.Chem.* 72:7497-7503.

Ronaghi, M., M. Uhlen, and P. Nyren. 1998. A sequencing method based on real-time pyrophosphate. *Science.* 281:363, 365.

Rostami, A., C.J. Wei, G. Guerin, and M.S. Taylor. 2011. Anion detection by a fluorescent poly(squaramide): self-assembly of anion-binding sites by polymer aggregation. *Angew.Chem.Int.Ed Engl.* 50:2059-2062.

Russell, R.G.G., S. Bisaz, A. Donath, D.B. Morgan, and H. Fleisch. 1971. Inorganic pyrophosphate in plasma in normal persons and in patients with hypophosphatasia, osteogenesis imperfecta, and other disorders of bone. *J.Clin.Invest.* 50:961-969

Ryan, L.M., R.L. Wortmann, B. Karas, M.P. Lynch, and D.J. McCarty. 1986. Pyrophosphohydrolase activity and inorganic pyrophosphate content of cultured human skin fibroblasts. Elevated levels in some patients with calcium pyrophosphate dihydrate deposition disease. *J.Clin.Invest.* 77:1689-1693.

Sarpel, G., A. N. Barr, H.J. Lubansky, and A. Omachi. 1982. Erythrocyte phosphate content in huntington's disease. *Neurosci Lett.* 31: 91-96.

Shin, I., S.W. Bae, H. Kim, and J. Hong. 2010. Electrogenerated chemiluminescent anion sensing: selective recognition and sensing of pyrophosphate. *Anal.Chem.* 82:8259-8265.

Su, X., C. Zhang, X. Xiao, A. Xu, Z. Xu, and M. Zhao. 2013. A kinetic method for expeditious detection of pyrophosphate anions at nanomolar concentrations based on a nucleic acid fluorescent sensor. *Chem. Commun.* 49:798-800.

Terkeltaub R.A., M. Rosenbach, F. Fong, and J. Goding. 1994. Causal link between nucleotide pyrophosphohydrolase overactivity and increased intracellular inorganic pyrophosphate generation demonstrated by transfection of cultured fibroblasts and osteoblasts with plasma cell membrane glycoprotein–1.*Arthritis&Rheumatism*. 37:934-941.

Terkeltaub R.A. 2001. Inorganic pyrophosphate generation and disposition in pathophysiology. *Am.J.Physiol.CellPhysiol.* 281:C1-C11.

Wright, G.D., and M. Doherty. 1997. Calcium pyrophosphate crystal deposition is not always 'wear and tear' or aging. *Ann.Rheum.Dis.* 56:586-588.

Xu, S., M. He, H. Yu, X. Cai, X. Tan, B. Lu, and B. Shu. 2001. A quantitative method to measure telomerase activity by bioluminescence connected with telomeric repeat amplification protocol. *Anal.Biochem.* 299:188-193.

Xu, S.Q., M. He, H.P. Yu, X.Y. Wang, X.L. Tan, B. Lu, X. Sun, Y.K. Zhou, Q.F. Yao, Y.J. Xu, and Z.R. Zhang. 2002. Bioluminescent method for detecting telomerase activity. *Clin.Chem.* 48:1016-1020.

Zapata, F., A. Caballero, N.G. White, T.D.W. Claridge, P.J. Costa, V. Felix, and P.D. Beer. 2012. Fluorescent charge-assisted halogen-bonding macrocyclic halo-imidazolium receptors for anion recognition and sensing in aqueous media. *J.Am.Chem.Soc.* 134:11533-11541.

8. Appendix:

PiPer™ Pyrophosphate Assay Kit (Life Technologies): Dilution Tables for Stock solution preparations.

Table A1 Sample Preparations for the standard curve preparation using PiPer™ Pyrophosphate Assay Kit (*Life Technologies*). Stock solutions were diluted as required for the ease of pipetting.

Components	Amount	Diluted in 1X Reaction Buffer	Final solution Concentration	Final Solution Volume
50mM Pyrophosphate (Component I) **[Negative ctrl]**	0 μl	50 μl	0 μM	50 μl
50mM Pyrophosphate (Component I)	0.01 μl	49.99 μl	10 μM	50 μl
50mM Pyrophosphate (Component I)	0.02 μl	49.98 μl	20 μM	50 μl
50mM Pyrophosphate (Component I)	0.03 μl	49.97 μl	30 μM	50 μl
50mM Pyrophosphate (Component I)	0.04 μl	49.96 μl	40 μM	50 μl
50mM Pyrophosphate (Component I)	0.05 μl	49.95 μl	50 μM	50 μl
20mM H_2O_2**[Positive ctrl]**	0.025 μl	49.97 μl	10 μM	50 μl

Table A2 Component wise amounts of working solution used for PPi measurement for 1 assay using PiPer™ Pyrophosphate Assay Kit (*Life Technologies*). Stock solutions were diluted as required for the ease of pipetting.

Components	1 Assay
1X Reaction Buffer	0.0468 ml=46.8 μl
100 uM Amplex Red reagent	0.5 μl
0.02 U/ml Inorganic pyrophosphatase	0.5 μl
4 U/ml maltose phopshorylase	1 μl
2 U/ml glucose oxidase	0.5 μl
0.4 U/ml HRP	0.2 μl
0.4 mM Maltose	0.5 μl
Total Volume	50 μl

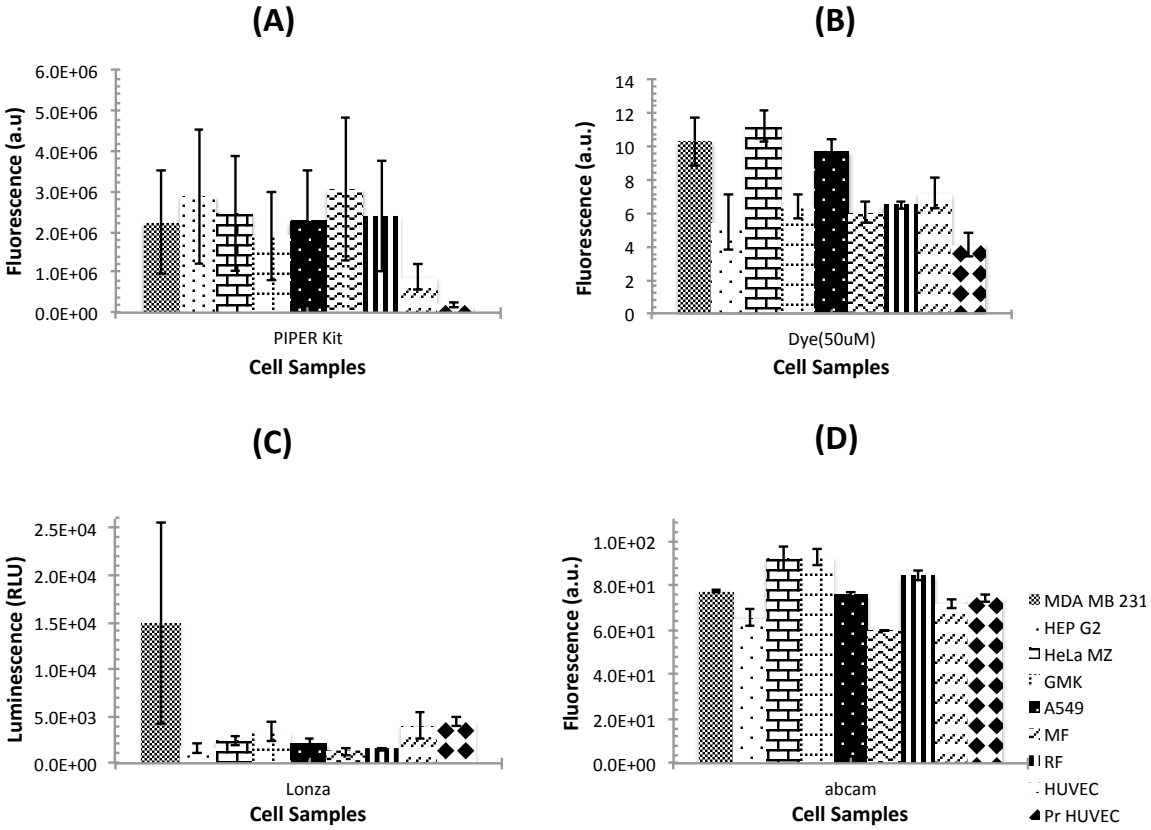

Fig. A3 Fluorescence and Luminescence obtained from unknown amounts of cell homogenates' concentration when investigated with commercial kits (A) PiPer^{TM} Pyrophosphate Assay Kit (*Life Technologies*), (B) 50 μM $ZnCl_2L$ probe, (C) PPiLight^{TM} Inorganic Pyrophosphate Assay (*Lonza*) and (D) Pyrophosphate Assay Kit, Fluorometric (*ab112155, Abcam*). PPi content was measured by exciting the samples at 485 nm and 340 nm respectively with *Victor^{TM} XM4 2030 Multilabel Reader* (*Perkin Elmer*) for PIPER and Abcam kits. In the case of $ZnCl_2L$ probe *Varian Cary Eclipse* Spectrophotometer was used to excite the samples at 440 nm with an emission around 591 nm. Luminescence with Lonza kit was read with 0.1 s integrated time. The values given here are the mean representation of three repeats (±Std Error).

Table A4 BSA standard concentrations for standard curve in Bradford Assay

BSA (μl)	dH_2O (μl)	BioRad Reagent (μl)
100	700	200
200	600	200
300	500	200
400	400	200
500	300	200